Progress In Electromagnetics Research Letters, Vol. 85, 91–99, 2019

Design and Development of Recessed Ground Microstrip Line Low Pass Filters

Anushruti Jaiswal*, Mahesh P. Abegaonkar, and Shiban K. Koul

Abstract—The design of conventional stepped-impedance microstrip line low pass filter (LPF) is based on high (Z_H) to low impedance (Z_L) ratio. The width of Z_H line, for $Z_H > 100\,\Omega$, becomes critical and challenging, especially on high dielectric constant substrates. A concept of air-filled recessed ground plane below a microstrip line is introduced in this paper. The effect of dimensions of recessed ground on characteristic impedance, attenuation, and propagation constant of a microstrip line are first studied. This simple approach is utilized to design the Z_H line of stepped-impedance microstrip line LPFs. Prototypes of recessed ground stepped-impedance microstrip line LPFs with Z_H/Z_L (keeping Z_L constant as $20\,\Omega$) ratio in the range 6 to 10 are designed and developed on Rogers 4350B of height 0.508 mm with $\varepsilon_r = 3.66$ at 3 GHz. For LPF with $Z_H/Z_L = 10$, the measured 3-dB cutoff frequency (f_c) is achieved at 3.12 GHz with return loss (RL) > 12 dB and insertion loss (IL) < 0.28 dB in its passband whereas the stopband attenuation (SBA) is better than 38 dB. In comparison to recessed ground LPF, the simulated results of conventional LPF with $Z_H/Z_L = 10$ (critical width of Z_H line =) are as follows RL > 10 dB and IL < 1.07 dB in passband at $f_c = 3$ GHz. The size of recessed ground LPF is reduced by 25%, when Z_H/Z_L is increased to 10 from 6. The approach of recessed ground microstrip line avoids the fabrication issues, reduces size, and improves the performance of LPF, which in turns confirms the advantages of recessed ground over conventional microstrip line.

1. INTRODUCTION

Low pass filters (LPF) are indispensable component of a microwave communication system. They are used for frequency selectivity by removing the undesired harmonics. Stepped impedance LPFs are commonly used for this purpose. They are also known as Hi-impedance and Low-impedance filters. Conventionally, these filters have gradual cutoff response in the stopband. By increasing number of sections, the rejection characteristics can be improved. However, increasing number of sections increases passband insertion loss (IL) and the physical size of the filter. Several techniques have been reported to address these problems. In [1, 2], low pass filters (LPFs) employing complimentary split ring resonator (CSRRs) structures in the ground planes are proposed to achieve a sharp rejection response. Defected ground plane LPFs with dumb-bell shaped [3], Hilbert curve ring shaped [4] and metal loaded structures [5] are suggested to reduce the size of the filter and attain a sharp cutoff frequency response in the stopband. UDSRC (unipolar double spiral resonant cell) [6], multiband meandered slotted ground plane resonator [7], and quarter wave stepped-impedance resonator [8] are also used to achieve sharp-rejection in LPF.

Micromachining is also a popular approach utilized in [9, 10] that extends the useful range of high- and low-impedance values in microstrip on high dielectric-constant materials and helps in attaining a sharp rejection band edges.

Received 3 April 2019, Accepted 22 May 2019, Scheduled 23 June 2019
* Corresponding author: Anushruti Jaiswal (anushruti88jaiswal@gmail.com).
The authors are with the Indian Institute of Technology, India.

In this paper, a recessed ground plane technique is proposed to design stepped-impedance microstrip line LPFs possessing low insertion loss, high rejection stopband and compact size. This technique is much simpler to implement and has lower fabrication cost than other techniques reported. The ratio of high impedance and low impedance (Z_H/Z_L) lines should be kept as high as possible for better approximation of lumped element capacitor and inductor realization. In general, the Z_H/Z_L line for conventional stepped-impedance LPF is 5 ($20\,\Omega$: $100\,\Omega$) [9]. It is chosen considering the issues of occurrence of transverse resonance at operating frequency due to width of low impedance line and fabrication limitations of high impedance line width. In some cases, passive circuits like filters are preferred to be designed on high index substrates (silicon ($\varepsilon_r - 11.7$), GaAs ($\varepsilon_r - 12.9$), alumina ceramic ($\varepsilon_r - 9.8$)), which further becomes more challenging, to physically realize the high impedance lines. However, in the proposed filter designs, a low impedance line of $20\,\Omega$ (implying in the conventional way) is used whereas a high impedance line of maximum $200\,\Omega$ is realized using a line of typically $50\,\Omega/20\,\Omega$ (on conventional ground plane) with recessed ground plane. The significance of choosing $50\,\Omega/20\,\Omega$ line with recessed ground for designing these filters will be explained further in the following sections. The characteristic impedance of recessed ground line can be controlled by the dimensions of recessed ground. Hence, as a proof of concept, recessed ground LPFs with Z_H/Z_L of 6, 7.5, and 10 are designed, fabricated, and characterized on a 0.508 mm RO4350B substrate with permittivity of 3.66 at 3 GHz. In the Z_H/Z_L, Z_L is always kept fixed as $20\,\Omega$, whereas Z_H is increased up from $120\,\Omega$ to till $200\,\Omega$. As Z_H/Z_L increases, the insertion loss in passband and the size of filter decrease. A lower dielectric constant substrate is chosen for demonstration of the concept because of limited resources available.

The paper is divided into three sections. Section 2 details the design and effect of dimensions of recessed ground on the characteristics of a microstrip line. Section 3 illustrates the design details, fabrication, and measured results of all the proposed variant prototypes of LPFs. Section 4 concludes the proposed work.

2. STRUCTURAL CONFIGURATION OF RECESSED GROUND MICROSTRIP LINE

Figures 1(a) and (b) illustrate the cross-sectional and perspective view of the recessed ground microstrip line, respectively. It is composed of a 50-Ω transmission line, substrate, and recessed ground plane. The microstrip line of width 1.127 mm (m_w) is designed on a 0.508 mm (t_{sub}) thick Rogers 4350B substrate with relative permittivity $\varepsilon_r = 3.66$. An air-filled recessed ground plane of aluminium material is present below the substrate. The dimensions of recessed ground include its width (a) and depth (t_{air}). They control the characteristic impedance (Z_c) and propagation constant (β) of the transmission line. The total height of the mixed air-substrate is $t = t_{air} + t_{sub}$ whereas the total height of recessed ground plane is t_1.

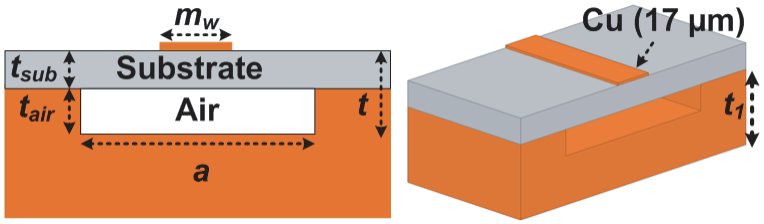

Figure 1. (a) Cross-sectional and (b) perspective view of recessed ground microstrip line.

Full wave FEM simulations of recessed ground microstrip line are carried out using ANSYS software (HFSS-High Frequency Structure Simulator). Parametric variation of a and t_{air} are done. The width (a) extends beyond m_w from 5 mm to 40 mm in steps of 5 mm at different values of t_{air}. The dimension of m_w remains constant. The variations of characteristic impedance (Z_c), attenuation constant (α), and normalized propagation constant ($\beta/k_0 = \sqrt{\varepsilon_{eff}}$) as a function of a and t_{air} are shown in Figure 2. From Figure 2(a), it is observed that Z_0 increases with increase in a for all the values of t_{air}. It also

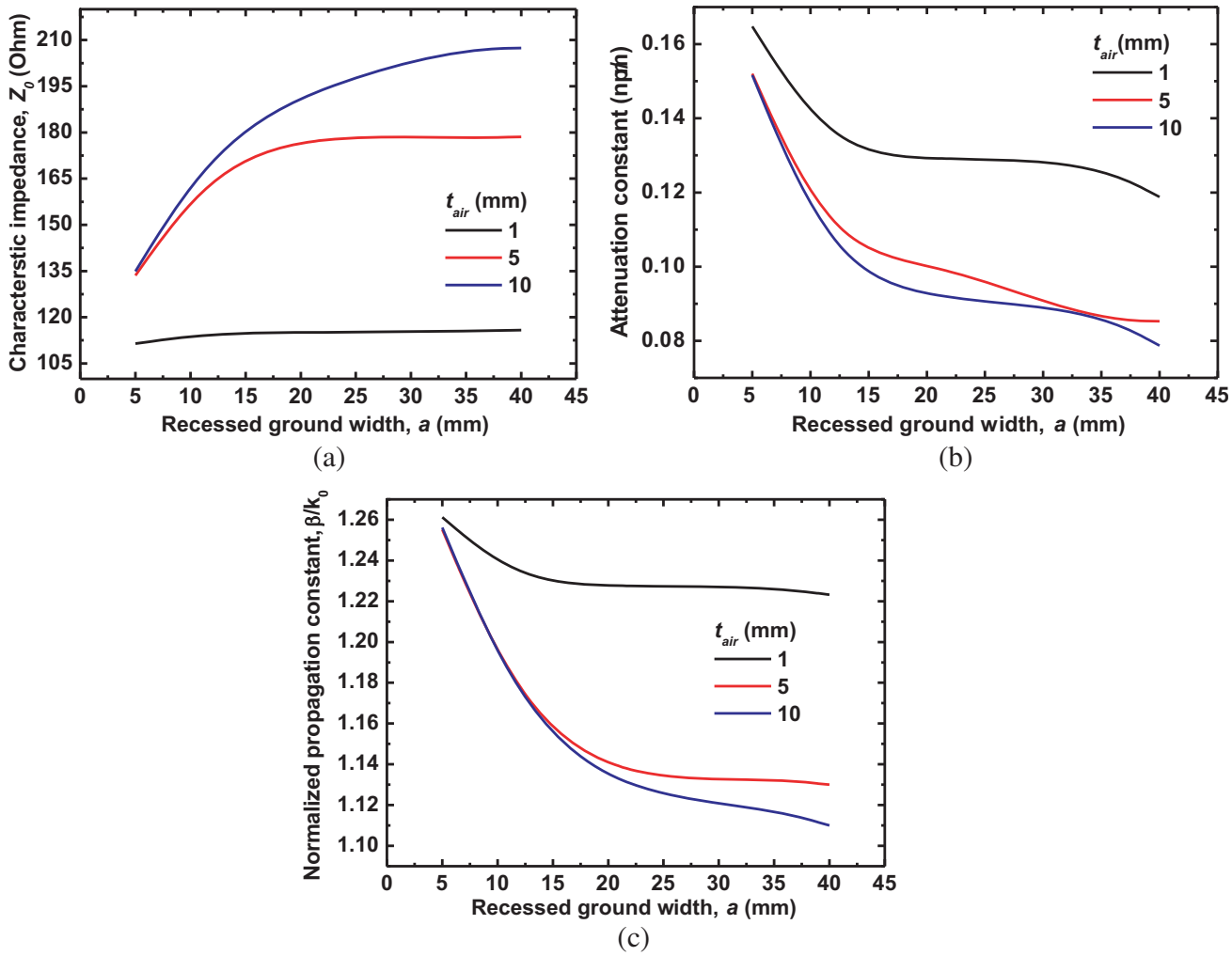

Figure 2. Variation of (a) characteristic impedance (b) attenuation and (c) normalized propagation constant as a function of a and t_{air} at $m_w = 1.127\,\text{mm}$ ($50\,\Omega$).

increases with increase in t_{air} and reaches maximum of $205\,\Omega$ at $a = 40\,\text{mm}$, $t_{air} = 10\,\text{mm}$. In Figure 2, it can be noticed that α (refer Figure 2(b)) and β/k_0 (refer Figure 2(c)) decrease with increase in a and t_{air}. α and β/k_0 reach minimum values of $0.078\,\text{Np/m}$ and 1.11 at $a = 40\,\text{mm}$ and $t_{air} = 10\,\text{mm}$. The presence of mixed air-substrate region below the microstrip line increases Z_c, decreases attenuation constant and effective dielectric constant by reducing the dielectric losses in the structure. The change in Z_c, α and β/k_0 almost saturates for $a > 35\,\text{mm}$ for all the values of t_{air}.

The equivalent circuit model of recessed ground microstrip line would remain identical to conventional microstrip line, as shown in [11–13]. From [11], it can be observed that all the lumped element components except R (equivalent resistance in ohms) depend on ε_{eff} and Z_c. It is understood from Figures 2(a) and (c) that Z_c and ε_{eff} of recessed ground microstrip line vary with the change in parameters a and t_{air}. Hence, the values of lumped component L (equivalent inductance in henry), G (equivalent conductance in mho), and C (equivalent capacitance in farad) would be different for conventional and recessed ground microstrip lines, but the value of R remains same.

3. RECESSED GROUND LOW PASS FILTERS

Recessed ground stepped-impedance Chebyshev-type microstrip line LPFs with different ratios of high to low impedance (Z_H/Z_L) are designed and fabricated on a 0.508 mm RO4350B substrate with

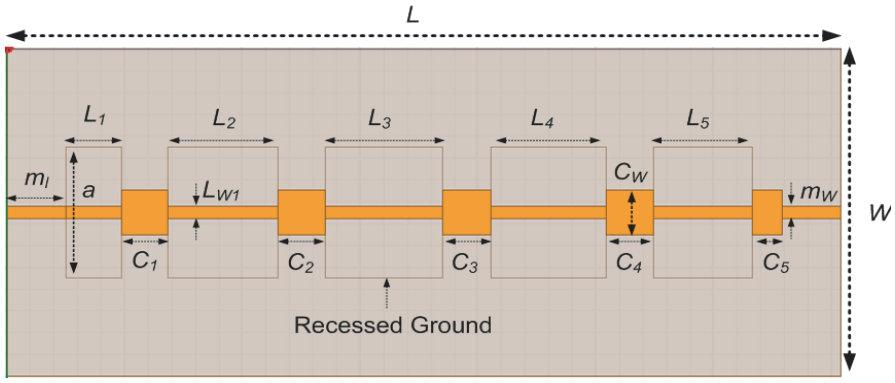

Figure 3. Layout of conventional stepped-impedance microstrip line low pass filter (case 1).

permittivity of 3.66. Conventional LPF design guidelines, as in [14], are used for designing purpose. Three filters with Z_H/Z_L as 6, 7.5, and 10 are designed for the following specifications: cutoff frequency, $(f_c) = 3\,\text{GHz}$, ripple in passband $(L_a) = 0.1\,\text{dB}$, frequency of attenuation, $(f_{atten}) = 4\,\text{GHz}$, attenuation at $f_{atten}(L) = 40\,\text{dB}$, and order of filter $(n) = 8$. Figure 3 shows the layout of recessed ground stepped-impedance LPF with its geometrical parameters. It is represented as case 1. The lumped element capacitor and inductor are realized as a low impedance (Z_L) line and a high impedance (Z_H) recessed ground line, respectively. The lengths of Z_L lines are denoted as C_n $(n = 1$ to $5)$ with their width $= C_W = 4.04\,\text{mm}$ whereas the recessed ground lines are represented as L_n $(n = 1$ to $5)$ with their width $= L_{W1} = m_w$. The recessed ground below the line has its dimensions as width (a) and depth (t_{air}) (seen from Figure 1). The parameter L_{W1} is kept equal to m_w to avoid step-discontinuity between them at both the ends, and in turn it reduces the loss. The length and width of $50\,\Omega$ line (source impedance) are $m_l = 5\,\text{mm}$ and $m_w = 1.127\,\text{mm}$. The overall size of the LPF is $L \times W$ where $W = 25\,\text{mm}$ and L is different for varying Z_H/Z_L.

In case 1, there is a step-discontinuity between L_{W1} and C_W which is more prominent than that between L_{W1} and m_w. Henceforth, in order to avoid this, another variant of recessed ground LPF is proposed as case 2, where parameter L_{W1} is kept equal to C_W, to maintain the uniformity and reduce the losses, as shown in Figure 4. Since C_W is larger than L_{W1}, the dimensions of recessed ground to realize Z_H values will increase correspondingly. In this paper, this type of filter is designed for only $Z_H/Z_L = 6$, i.e., $Z_H = 120\,\Omega$. It is difficult to realize $Z_H/Z_L > 6$ with case 2 on lower dielectric constant substrate, as used in this paper, because the parameters of recessed ground would become very large to achieve $Z_H \gg 6$ and further increase the overall size of filter. However, this concept is very useful for designing low loss and compact recessed ground LPFs on higher index substrates with $Z_H/Z_L \gg 6$.

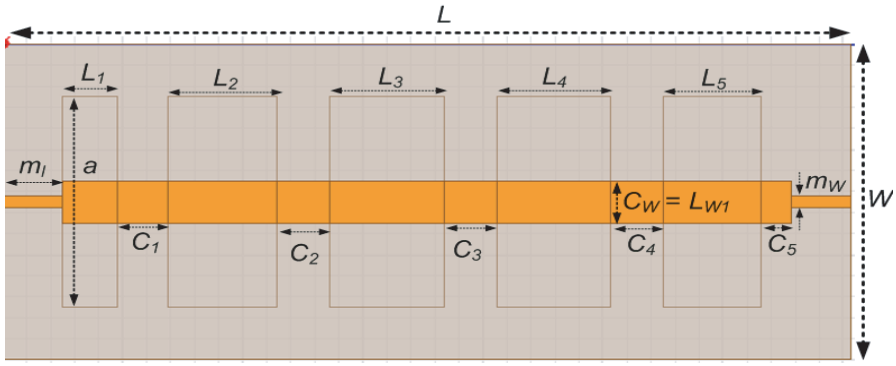

Figure 4. Layout of recessed ground stepped-impedance microstrip line low pass filter with $L_{W1} = C_W$ (case 2).

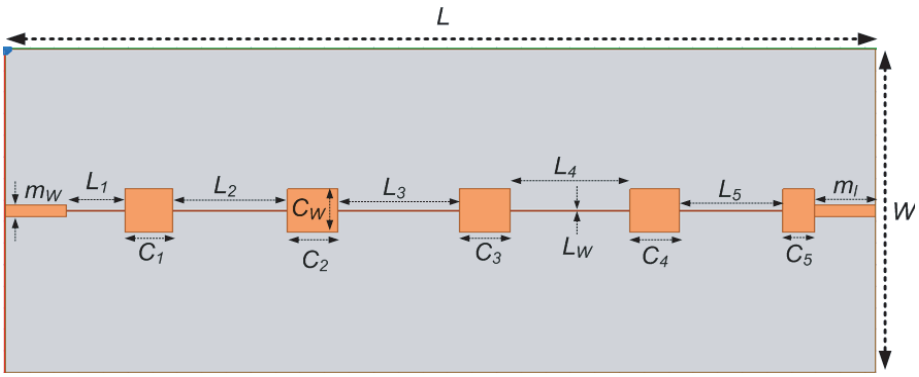

Figure 5. Layout of recessed ground stepped-impedance microstrip line low pass filter.

The performance of recessed ground LPFs of both cases are compared with simulated results of conventional LPFs, shown in Figure 5. No recessed ground is present below the Z_H lines. The lumped element capacitor and inductor are realized asa low impedance (Z_L) line and a high impedance (Z_H) line, respectively. The width of Z_H line (L_W) is different for varying Z_H/Z_L. Since the value of Z_L does not change, W_C remains constant. The lengths L_n and C_n are computed and mentioned in Table 1, for different Z_H/Z_L LPFs along with their total length (L). Since the values of Z_H are the same for case 1 and case 2, parameter L is approximately the same. However, for case 2, it is slightly smaller due to removal of the step-discontinuity. Comparing L of cases 1(a) and (c), the size of the filter is reduced by 25%.

Table 1. Length of inductor and capacitors for different Z_H/Z_L for $Z_L = 20\,\Omega$.

Length (mm)	$Z_H = 120\,\Omega$ ($Z_H/Z_L = 6$) **Case 1(a)**	$Z_H = 120\,\Omega$ ($Z_H/Z_L = 6$, $L_W = C_W$) **Case 2**	$Z_H = 150\,\Omega$ ($Z_H/Z_L = 7.5$) **Case 1(b)**	$Z_H = 200\,\Omega$ ($Z_H/Z_L = 10$) **Case 1(c)**
L_1	4.74	9.03	3.53	2.
L_2	9.33	9.55	6.603	4.56
L_3	9.90	9.43	6.889	4.74
L_4	9.78	8.13	6.832	4.71
L_5	8.40	4.56	6.059	4.24
C_1	3.89	4.20	4.27	4.52
C_2	4.09	4.41	4.735	5.17
C_3	4.10	4.43	4.78	5.20
C_4	0.88	4.34	4.603	4.97
C_5	2.54	2.53	2.602	2.68
L	**70.8**	**70.6**	**60.91**	**53.3**

The dimensions of recessed ground (a and t_{air}) and L_w for cases 1 and 2 are tabulated in Table 2. It can be noticed that the dimensions of recessed ground increase with an increase in Z_H, and comparing case 1(a) with case 2, the size is larger for case 2, as $C_W > m_w$. The width L_W decreases with increasing value of Z_H and is practically not realizable for case 1(c). The use of recessed ground makes it easier to design the LPF with high Z_H/Z_L.

The fabricated images of recessed ground filters are shown in Figure 6. Thick aluminium metal is used to design the recessed ground. The slots are created in aluminium using milling machine. The printed substrate is glued to recessed ground using silver conductive paste.

Table 2. Dimensions of recessed ground (a and t_{air}) and L_w to realize different Z_H/Z_L.

Recessed ground LPF ($L_{w1} = m_w = 1.127\,\text{mm}$)	$Z_H = 120\,\Omega$ Case-1(a)	$Z_H = 120\,\Omega$ Case-2, $L_{W1} = C_W$	$Z_H = 150\,\Omega$ Case-1(b)	$Z_H = 200\,\Omega$ Case-1(c)
a (mm)	12	20	21	34
t_{air} (mm)	1.25	5	2.471	10.876
Conventional LPF L_W (mm)	0.144	0.144	0.057	0.008

SMA connectors are used for the measurements. Figure 7 depicts the simulated and measured S-parameters of recessed ground LPFs of cases 1 and 2. The S-parameters of recessed ground LPFs are also compared with conventional LPFs for $Z_H/Z_L = 6$, 7.5, and 10 in Figures 7(a), (c), and (d), respectively. Figure 7(b) shows the simulated and measured results of recessed ground LPF for $Z_H/\text{Z}_L = 120\,\Omega$ with $L_W = C_W$. The measured results agree well with the simulated ones. The characteristics of recessed ground LPFs are stated and compared with conventional LPFs in Table 3. f_c of recessed ground filters are roughly close to 3 GHz (as in simulations) with a 100 MHz of shift in cases 1(b) and (c). The discrepancy can be accounted to undesired air-gap between the printed substrate and recessed ground

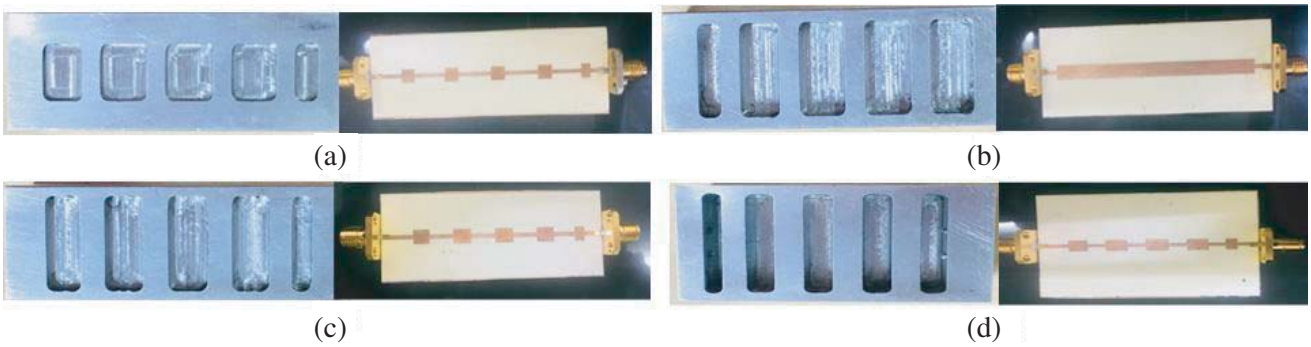

Figure 6. Top view of recessed ground (left) and recessed ground low pass filter (LPF) (right). (a) case 1: $Z_H = 120\,\Omega$, (b) case 2: $Z_H = 120\,\Omega$ with $L_W = C_W$, (c) case 1(b): $Z_H = 150\,\Omega$ and (d) case 1(c): $Z_H = 200\,\Omega$. For all the cases $Z_L = 20\,\Omega$.

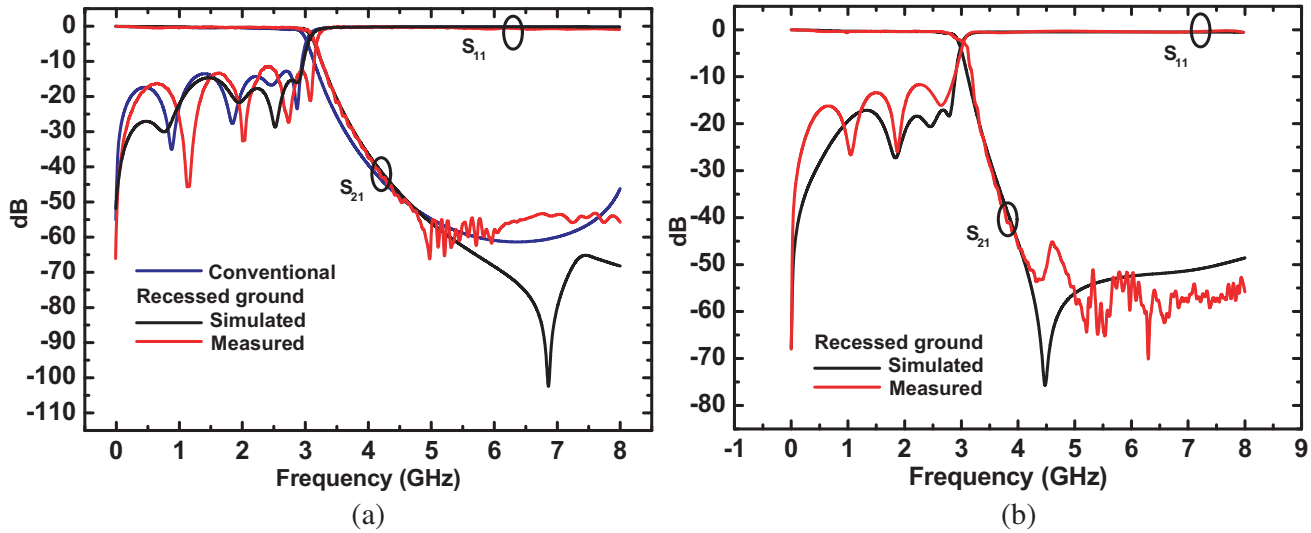

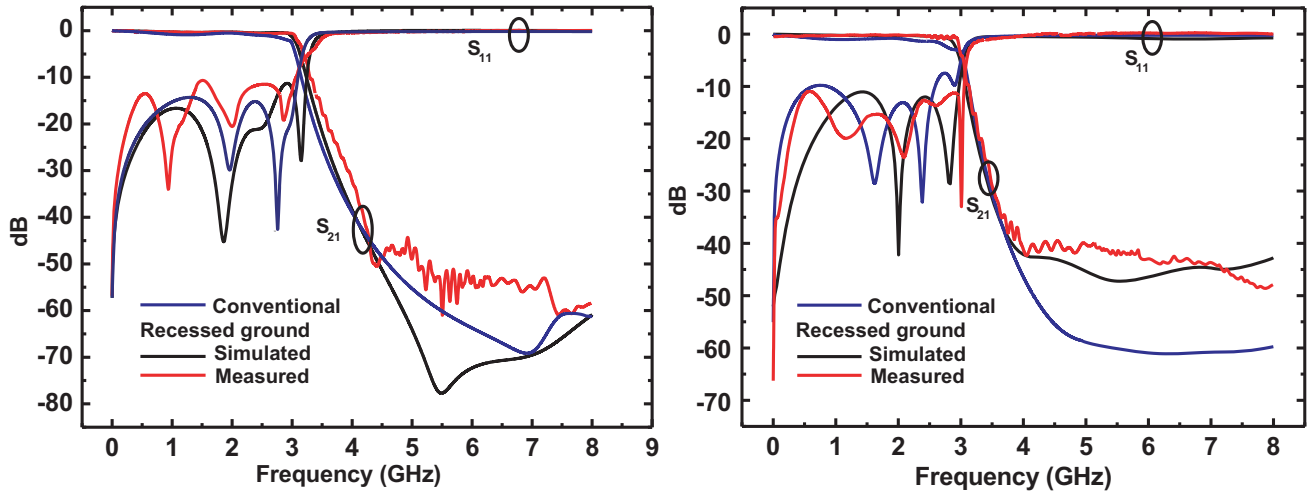

Figure 7. Simulated and measured S-parameters of recessed ground and conventional LPF's. (a) case 1: $Z_H = 120\,\Omega$, (b) case 2: $Z_H = 120\,\Omega$ with $L_W = C_W$, (c) case 1(b): $Z_H = 150\,\Omega$ and (d) case 1(c): $Z_H = 200\,\Omega$. For all the cases $Z_L = 20\,\Omega$.

due to silver conductive paste. The insertion loss (IL) decreases with an increase in the value of Z_H/Z_L. Least measured IL of 0.28 dB is achieved in case 1(c). It is 0.79 dB less than conventional LPF (case 1(c) — 1.07 dB — simulated). The IL in case 2 is slightly less than case 1(a), and it is concluded that recessed ground LPFs with uniform width lines reduce the step-discontinuity losses. The IL in conventional LPFs increases with an increase in Z_H because the width L_W decreases, and however, it increases the step-discontinuity losses between L_W and C_W. Comparing all the cases, the measured return loss in the passband is better than 12 dB whereas the attenuation in stopband is higher than 30 dB.

Table 3. Comparison of characteristics of recessed ground LPF's with conventional LPFs for different Z_H/Z_L.

	Recessed ground LPF (measured results)				Conventional LPF (simulated results)		
Parameters	Case-1(a)	Case-2	Case-1(b)	Case-1(c)	Case-1(a)	Case-1(b)	Case-1(c)
f_c (GHz)	3.08	2.98	3.1	3.12	3.03	3.09	3.1
Max. S_{21} (dB)	0.4	0.336	0.32	0.28	0.5	0.9	1.07
S_{11} (dB)	> 13	> 15	> 13	> 12	> 15	> 14	> 10
L (dB) at f_{atten}	35	40	30	38	40	40	40

The performance of proposed LPF in case 1(c) is compared with some of the existing planar LPFs in Table 4. The EL of proposed LPF is longer than that of all the other reported works (except [5]). However, $|S_{21}|$ (dB) in passband of the proposed LPF is much less than other LPFs. The stopband attenuation ($|S_{21}|$ (dB)) is also better than all the reported works. Hence, it can be concluded that the recessed ground technique has less losses.

The performance of proposed LPF (case 1(c)) is compared with other existing planar LPFs in Table 4. From Table 4, it can be observed that even though there is longer EL in proposed work than other reported works, the insertion loss is least for the proposed LPF. Hence, it can be concluded that recessed ground microstrip line possesses lower losses than conventional microstrip line. The stopband attenuation is also better for recessed ground LPF than other works.

Table 4. Comparison of proposed LPF in case 1(c) with other existing planer LPFs.

Ref.	f_c (GHz)	Passband $\|S_{11}\|$ (dB)	Passband $\|S_{21}\|$ (dB)	EL* (in terms of λ_g)	Stopband $\|S_{21}\|$ (dB)
[1]	1.89	> 14	< 0.5	$0.23\lambda_g$	> 20
[2]	2.2	> 20	< 0.9	$0.263\lambda_g$	> 20
[3]	2.2	> 11	< 0.5	$0.26\lambda_g$	> 20
[4]	2.3	> 9	< 0.5	1.2 λ_g	> 33
[5]	2.4	> 10	< 0.9	1.07 λ_g	> 20
[6]	1.9	> 8	< 2	$0.61\lambda_g$	> 10
[7]	2.9	> 10	< 0.7	$20\times$	> 20
[8]	5.05	> 12	< 0.8	$0.68\lambda_g$	> 19.5
This work	**3.12**	**> 12**	**< 0.28**	**$1.02\boldsymbol{\lambda_g}$**	**> 38**

EL* — Port to port electrical length in terms of guided wavelength at 3-dB cutoff frequency.

4. CONCLUSION

A concept of recessed ground microstrip line is introduced to design a compact stepped-impedance LPF with low insertion loss and high stopband attenuation. This approach is much simpler to implement and cost effective to fabricate than other reported techniques. A stepped impedance microstrip line LPF at 3 GHz, for $Z_H/Z_L = 10$ is designed and developed using recessed ground. A maximum measured insertion loss of 0.28 dB, return loss better than 12 dB in passband, and rejection better than 38 dB in stopband are achieved. The insertion loss is 0.79 dB less than the simulated insertion of conventional LPF with $Z_H/Z_L = 10$. The size of filter is miniaturized by 25% in comparison to LPF with $Z_H/Z_L = 6$. The results of recessed ground filter validates the concept and concludes the following advantages: 1. Lower insertion loss, 2. Miniaturization and 3. Sharp rejection response.

REFERENCES

1. Mandal, M. K., P. Mondal, S. Sanyal, and A. Chakrabarty, "Low insertion-loss, sharp-rejection and compact microstrip low-pass filters," *IEEE Microwave and Wireless Components Letters*, Vol. 16, No. 11, 600–602, Nov. 2006.
2. Zhang, J., B. Cui, S. Lin, and X.-W. Sun, "Sharp-rejection low-pass filter with controllable transmission zero using Complementary Split Ring Resonators (CSRRs)," *Progress In Electromagnetics Research*, Vol. 69, 219–226, 2007.
3. Chen, Z.-Y., L. Li, and S.-S. Chen, "A novel dumbbell-shaped defected ground structure with embedded capacitor and its application in low-pass filter design," *Progress In Electromagnetics Research Letters*, Vol. 53, 121–126, 2015.
4. Chen, J., Z.-B. Weng, Y.-C. Jiao, and F.-S. Zhang, "Low pass filter design of Hilbert curve ring defected ground structure," *Progress In Electromagnetics Research*, Vol. 70, 269–280, 2007.
5. Kumar, A., et al., "Design of nine pole microstrip low pass filter with metal loaded defected ground structure," *2016 IEEE MTT-S Latin America Microwave Conference (LAMC)*, 1–3, Puerto Vallarta, 2016.
6. Lu, K., G.-M. Wang, Y.-W. Wang, and X. Yin, "An improved design of Hi-LO microstrip lowpass filter using uniplanar double spiral resonant cells," *Progress In Electromagnetics Research Letters*, Vol. 23, 89–98, 2011.
7. Wang, C. J. and T. H. Lin, "A multi-band meandered slotted-groundplane resonator and its application of low-pass filter," *Progress In Electromagnetics Research*, Vol. 120, 249–262, 2011.

8. Jiang, M. and W. Hong, "An approach for improving the transition-band characteristic of a stepped-impedance low-pass filter," *2012 International Conference on Microwave and Millimeter Wave Technology (ICMMT)*, 1–4, Shenzhen, 2012.
9. Drayton, R. F., S. Pacheco, J. G. Yook, and L. P. B. Katechi, "Micromachined filters on synthesized substrates," *1998 IEEE MTT-S International Microwave Symposium Digest (Cat. No. 98CH36192)*, Vol. 3, 1185–1188, Baltimore, MD, USA, 1998.
10. Sharma, P., S. K. Koul, and S. Chandra, "Design and development of microstrip low pass filters at K-band using MEMS technology," *2007 Asia-Pacific Microwave Conference*, 1–4, Bangkok, 2007.
11. Eudes, T., B. Ravelo, and A. Louis, "Transient response characterization of the high-speed interconnection RLCG-model for the signal integrity analysis," *Progress In Electromagnetics Research*, Vol. 112, 183–197, 2011.
12. Ravelo, B., "Modelling of asymmetrical interconnect T-tree laminated on flexible substrate," *Eur. Phys. J. Appl. Phys. (EPJAP)*, Vol. 72, No. 2, 1–9, id 20103, Nov. 2015.
13. Eudes, T. and B. Ravelo, "Analysis of multi-gigabits signal integrity through clock H-tree," *International Journal of Circuit Theory and Applications (Int. J. Circ. Theor. Appl.)*, Vol. 41, No. 5, 535–549, May 2013.
14. http://ntuemc.tw/upload/file/20110321102525847f2.pdf.